2008-0592

46th Annual Fluid Dynamics Conference, January, Reno, NV

Effect of Freestream Noise on Roughness-Induced Transition for the X-51A Forebody

Matthew P. Borg,* Steven P. Schneider,† and Thomas J. Juliano‡

Purdue University, West Lafayette, IN, 47097-1282, USA

A 20%-scale X-51A forebody model was tested in the Boeing/AFOSR Mach-6 Quiet Tunnel. Repolishing the nozzle throat has restored quiet flow at high Reynolds numbers. The effect of a smooth blank and two different trip strips on windward-forebody transition was measured using temperature-sensitive paint and hot-wire anemometry. Reducing freestream noise from conventional to quiet levels increased the smooth-wall transition Reynolds number by a factor of at least 2.2. In addition, the transition Reynolds number based on the distance from the trips increased by a factor of 2.4 for the smaller trips and by a factor of 1.7 for the larger trips. Thus, tunnel noise had a substantial effect on roughness-induced transition.

I. Hypersonic Laminar-Turbulent Transition

Laminar-turbulent transition in hypersonic boundary layers is important for prediction and control of heat transfer, skin friction, and other boundary layer properties. Vehicles that spend extended periods at hypersonic speeds may be critically affected by the uncertainties in transition prediction, depending on their Reynolds numbers. Although slender vehicles are the primary concern, blunt vehicles are also affected by transition.[1] However, the mechanisms leading to transition are still poorly understood, even in low-noise environments.

Many transition experiments have been carried out in conventional ground-testing facilities over the past 50 years.[2] However, these experiments are contaminated by the high levels of noise that radiate from the turbulent boundary layers normally present on the wind tunnel walls.[3] These noise levels, typically 0.5-1% of the mean, are an order of magnitude larger than those observed in flight.[4,5] These high noise levels can cause transition to occur an order of magnitude earlier than in flight.[3,5] In addition, the mechanisms of transition operational in small-disturbance environments can be changed or bypassed altogether in high-noise environments; these changes in the mechanisms change the parametric trends in transition.[4] Mechanism-based prediction methods must be developed, supported in part with measurements of the mechanisms in quiet wind tunnels.

II. Development of Quiet-Flow Wind Tunnels

Only in the last two decades have low-noise supersonic wind tunnels been developed.[3,6] This development has been difficult, since the test-section wall boundary-layers must be kept laminar in order to avoid high levels of eddy-Mach-wave acoustic radiation from the normally-present turbulent boundary layers. A Mach-3.5 tunnel was the first to be successfully developed at NASA Langley.[7] NASA also operated a prototype quiet Mach 6 facility through 1995. It was removed from service due to operational conflicts and changing research priorities. The facility is now housed at Texas A&M. The Langley Mach-6 tunnel was used as a starting point for the new Purdue nozzle.[8] The Purdue Mach-6 tunnel is presently the only operational hypersonic quiet tunnel, anywhere in the world. Further details regarding the development of quiet hypersonic tunnels can be found in Ref. 9.

*Research Assistant, Student Member AIAA.

†Professor, Associate Fellow AIAA.

‡Research Assistant, Student Member AIAA

III. The Boeing/AFOSR Mach-6 Quiet Tunnel

Quiet facilities require low levels of noise in the inviscid flow entering the nozzle through the throat, and laminar boundary layers on the nozzle walls. To reach these low noise levels, conventional blow-down facilities must be extensively modified. Requirements include a 1 micron particle filter, a highly polished nozzle with bleed slots for the contraction-wall boundary layer, and a large settling chamber with screens and sintered-mesh plates for noise-reduction.[3] To reach these low noise levels in an affordable way, the Purdue facility, the Boeing/AFOSR Mach-6 Quiet Tunnel (BAM6QT), has been designed as a Ludwieg tube.[10] A Ludwieg tube is a long pipe with a converging-diverging nozzle on the end, from which flow exits into the nozzle, test section, and second throat (Figure 1). Care is taken to keep the air in the tunnel as dry as possible to avoid water condensation in the nozzle. The dewpoint of the air in the tunnel, measured with a Panametrics Moisture Target Series-5 dewpoint meter, was typically on the order of $-20°$C.

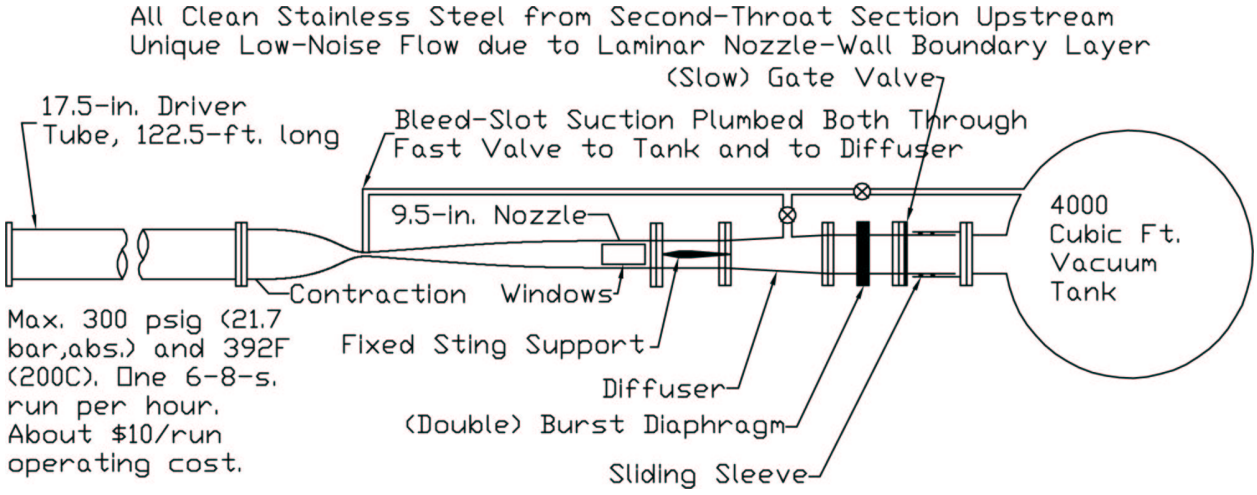

Figure 1: Schematic of Boeing/AFOSR Mach-6 Quiet Tunnel

A pair of diaphragms is placed downstream of the test section. When the diaphragms burst, an expansion wave travels upstream through the test section into the driver tube. Since the flow remains quiet after the wave reflects from the contraction, sufficient vacuum can extend the useful runtime to many cycles of expansion-wave reflection, during which the pressure drops quasi-statically.

The contraction-wall boundary layer is bled off just upstream of the throat, beginning a fresh undisturbed boundary layer for the nozzle wall. The nozzle-throat bleed air can be ducted to two alternate locations. A fast valve remains connected directly between the bleeds and the vacuum tank, allowing the bleed air to be dumped directly into the tank. In addition, the original plumbing connecting the bleed air to the diffuser enables a faster startup, if the jets of air into the diffuser are not a problem.

Figure 2 shows the nozzle. Here, z is an axial coordinate whose origin is at the nozzle throat. The region of useful quiet flow lies between the characteristics marking the onset of uniform flow, and the characteristics marking the upstream boundary of acoustic radiation from the onset of turbulence in the nozzle-wall boundary layer. A 7.5-deg. sharp cone is drawn on the figure. The rectangles are drawn on the nozzle at the location of window openings, all but one of which are presently filled with blank metal inserts. Images of the tunnel are available at `http://roger.ecn.purdue.edu/~aae519/BAM6QT-Mach-6-tunnel/`, along with earlier papers and other documentation.

IV. Status of Tunnel Performance

Tunnel performance from February 2005 through December 2006 is reported in Reference 11. Performance from January to April 2007 is reported in Reference 12.

The air compressor for the BAM6QT failed in late April, 2007. No runs were conducted for two months until late June, while a replacement air compressor was purchased and installed. There was no change in tunnel quiet performance after the extended downtime. The maximum quiet pressure was P_0=95 psia. Two runs at very high pressure (initial P_0 >250 psia) were conducted, with the intention of blowing dust out of

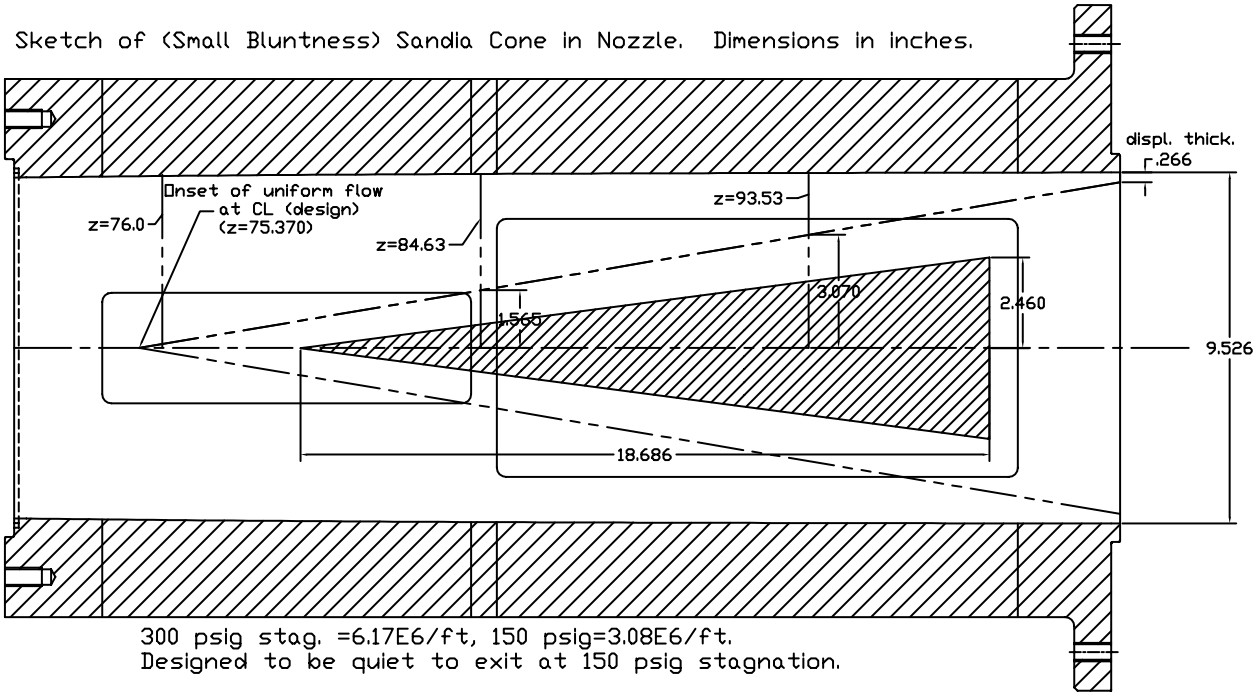

Figure 2: Schematic of Mach-6 Quiet Nozzle with Model

the nozzle. However, there was no change in maximum quiet pressure after these runs.

The nozzle was detached both at the throat and 30 in. downstream of the throat, twice in each case, for careful cleaning of this nozzle segment. No scratches were evident. Some dust was present and was removed as thoroughly as possible. After the first cleaning, the maximum quiet pressure dropped to 66 psia. The second cleaning resulted in a quiet pressure of 73 psia.

A third cleaning was conducted on August 2 and achieved a small increase in quiet pressure to 80 psia. On this occasion, two roughly-circular, approximately 1/16 in.-diameter spots were noticed at about 5 o'clock, 3 in. from the lip (2 in. behind the throat). They felt smooth to the touch and did not change when cleaned with acetone. Photos were taken, but they did not come out well due to the curved, highly-polished surface.

The electroformed nickel and steel nozzle was swapped out for the aluminum surrogate nozzle on August 24. Upon a close inspection of the electroformed nozzle, a scratch was noticed about 2 in. from the bleed lip between 7 and 8 o'clock. It was 0.3–0.5 in. long and parallel to the flow. Another mark was noticed at 12 o'clock, not far past the throat. It felt smooth and might have only been a discoloration. It was approximately 0.2 x 0.4 in. and perpendicular to the flow. The two small spots noticed before were still present and unchanged. The maximum quiet pressure of the surrogate nozzle was 60 psia.

While the BAM6QT continued to operate with the surrogate nozzle, the electroform was taken to Optek, Inc., the polisher that had done the previous work on the nozzle. They removed the scratch and other blemishes, which they described as corrosion marks. The nozzle was returned and reinstalled in late September. Initial tests demonstrated quiet flow when $P_0 < 140$ psia and several turbulent bursts (10–40 per run). Two high pressure runs had no effect on the performance. In the two months since installation, the maximum quiet pressure has decreased slightly to 135 psia and the number of turbulent bursts is typically about 3–8 per run, though occasionally there are closer to 30. This latest repolish of the nozzle achieved a substantial increase in performance, which has returned to about 90% of the target quiet pressure of 150 psia. However, the performance remains short of the previous record of 153 psia, perhaps due to imperfections in the surface finish.

V. Experiments on the X-51A Forebody

Purdue University is examining boundary-layer stability and transition on the X-51A forebody. The Purdue model is 20% scale for the portion of the vehicle forward of the engine inlet. Experiments using tem-

perature sensitive paint (TSP) and hot-wire anemometry were recently conducted to characterize the effect of tunnel noise on transition. These experiments were conducted on the windward side in the Boeing/AFOSR Mach-6 Quiet Tunnel (BAM6QT). When operated quietly, the nozzle-wall boundary layer remains laminar producing freestream noise levels on the order of 0.05%. When operated conventionally, the nozzle-wall boundary layer is turbulent and the noise level increases to about 3%.

For supersonic and hypersonic speeds, there have been only a few experiments that explore the effects of tunnel noise on roughness-induced transition.[4] Creel et al.[13] performed experiments on swept circular cylinders at Mach 3.5 under low freestream noise levels and also nearly-conventional levels. For the smooth-walled case, changing the tunnel noise levels was found to have no effect on transition. When small trips were added to the model, the transition Reynolds number was found to increase when the tunnel noise levels were decreased. Ito et al.[14] performed a low Reynolds number experimental study on a model of an axisymmetric scramjet forebody at Mach 4. The model included two compression corners. Data were collected with different-sized boundary-layer trips under low freestream noise levels and freestream noise levels approximately six times higher. Ito found that reducing the tunnel noise levels dramatically decreased intermittency and delayed transition significantly.

In order for the X-51A to operate as intended, the boundary layer entering the engine must be turbulent. This reduces the risk of unstart due to shock/boundary-layer interactions in the isolator and also allows more rapid mixing and burning within the combustor. To ensure a turbulent boundary layer, boundary layer trips must be added to the vehicle geometry upstream of the engine inlet. If the trips are too small, the boundary layer may remain laminar into the engine and prevent it from starting. If the trips are oversized, they will add unnecessary drag to the vehicle. Oversized trips may also reduce engine performance.

Such trips must be designed using empirical measurements. However, most hypersonic wind tunnels have turbulent wall boundary layers that radiate a good deal of acoustic noise into the flow. Given this inherent limitation of high-noise facilities, the effects of tripping should be evaluated in a low-noise environment in order to determine the effects of facility noise on transition.

The experiments reported here were all on the windward side of the model at an inviscid Mach number of 6.0 with an initial stagnation temperature of T_0=160°C at 4.0° angle of attack. The Purdue model consists of a stainless steel nose section with an aluminum afterbody, as shown in Figure 3. The model includes a nylon 6/6 insert on both the windward and leeward sides. The nylon inserts were included to act as a thermal insulator layer for temperature sensitive paint (TSP). Liu and Sullivan[15] present a good background of the physics of TSP. Matsumura[16] successfully employed the TSP technique on a generic scramjet forebody in the BAM6QT. The methodology used in the present experiments is very similar to his.

The assembled model is 13.55 in. long. The windward nylon insert is approximately 9.4 in. long and 1.0 in. wide. The insert is composed of a 0.4-in.-long flat surface followed by a compression corner. The remainder of the insert maintains a constant angle to the flow and a constant width. The nylon is coated with Ru(bpy) luminophore molecules in DuPont ChromaClear paint. It was calibrated to give quantitative surface temperatures. A photograph of the windward surface of the model is seen in Figure 3. For all of the data, the entire nylon insert was imaged. Flow is from left to right.

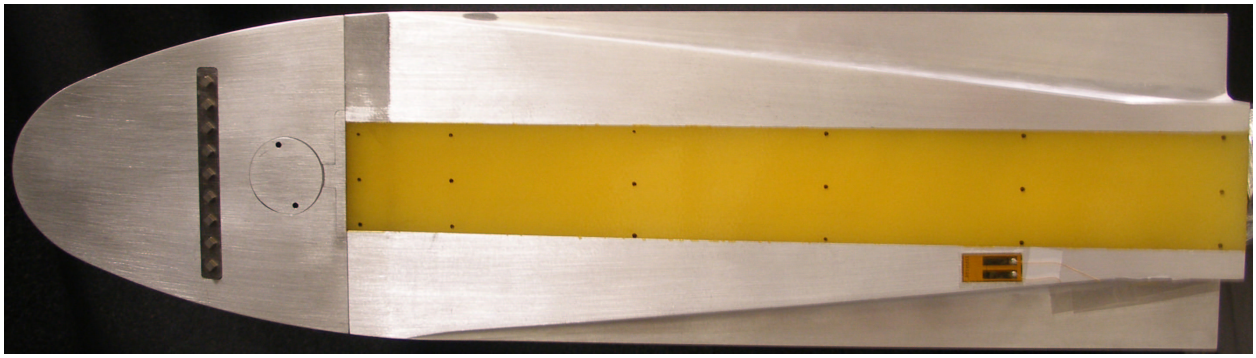

Figure 3: Photograph of windward side of model

A Photometrics SenSysB scientific-grade CCD camera was used to obtain all TSP images. Light at 464 nm from a 4-in. diameter ISSI LM4 blue LED array was used to excite the paint. During each TSP run, photographs were taken as fast as the hardware would allow, about one image every 600 ms. When the

oscilloscopes trigger, the camera begins taking pictures with a manually-set exposure length. The exposure was generally set to about 200 ms. The camera outputs a signal when the shutter is open. This signal was recorded and used in subsequent data processing to calculate Reynolds numbers for each image. The 'x' coordinates reported are not arclength, as the outer mold line data of the model have not been provided. Rather, they are a projection of the arclength onto a plane at 0° angle of attack above the model surface. Given the slight inclination of the model surface, using this definition of 'x' is not much different than using actual arclength.

A smooth strip and two trip strips with two different roughnesses were used in the model at a streamwise location of x=2.48 in. One of the trip strips is composed of diamond-shaped roughness elements while the other has ramp-shaped trips. A photograph of the three strips can be seen in Figure 4. The ramp roughnesses have the same shape as those used by Berry[17] on the Hyper-X model. Here, the flow is from top to bottom. The upstream edge of the ramp roughnesses are at the same height as the model surface. Moving downstream, they rise up above the model surface and also become increasingly narrow. At the downstream edge, the ramps have a maximum height of 0.030 in. Due to difficulties in getting the strip to fit in the model, a 0.005 in. shim was placed under the insert. This caused small forward-facing steps at both the upstream and downstream edges of the strip. A skilled machinist measured the step heights along the centerline and found them to be about 0.005 and 0.003 in., respectively. The diamond-roughness strip has diamond-shaped roughness elements which are 0.120-in.-wide across the diagonal and 0.060-in. high.

VI. Effect of Tunnel Noise

Runs were made with an initial stagnation pressure of 95 psia with all three inserts in the model. The tunnel was run under noisy and quiet conditions to assess the effects of noise on natural and roughness-influenced transition.

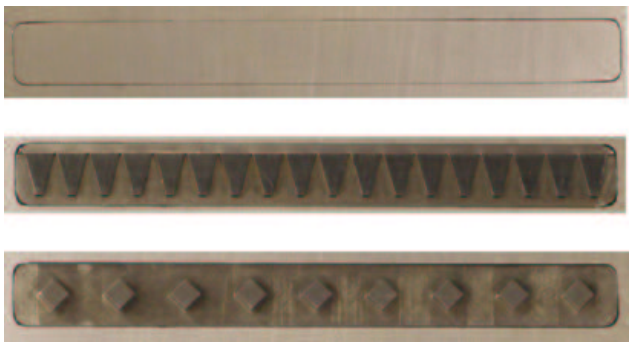

Figure 4: Trip inserts for model

It should be noted that when the tunnel is run noisy (with the throat bleed suction turned off), the total mass flux out of the driver tube decreases by about 38% from the bleeds-open case, the nozzle-wall boundary layer becomes turbulent, the flow becomes noisy, and the mean Mach number decreases from about 6.0 to about 5.8. This, in turn, means that the freestream Reynolds-number drop with time is less with the bleeds closed than with the bleeds open. This effect becomes important for the data that will be presented. When comparing data taken under noisy and quiet conditions, a choice needed to be made regarding whether to compare data at the same freestream Reynolds number or to compare data taken at the same time after the start of the run. The problem with comparing data at the same Reynolds number is that these data were taken at significantly different times during the run. It has been observed that over the course of a run, the mean temperature of the nylon increases. Additionally, there may also be non-negligible lateral heat conduction in the nylon. Thus, images taken at a time significantly into the run do not always accurately reflect the instantaneous surface conditions. It was therefore decided to compare data taken at similar times into a run. This leads to a small variation in Reynolds numbers when comparing these data.

In addition to the TSP data, an uncalibrated Dantec Dynamics hot film was located 10.5 in. downstream of the leading edge and about 1.25 in. off the centerline. The manufacturer-supplied temperature coefficient was 0.34%/°C. It was always operated with an in-house constant temperature anemometer (CTA) at an overheat ratio of 1.31, based on resistances, giving the film a temperature of 116°C. This hot film was used to determine if the boundary layer was laminar or turbulent. Schmisseur[18] et al. used a similar technique in Purdue's Mach-4 quiet tunnel. The data were recorded on a Textronix DPO7054 oscilloscope at a sampling rate of 2 million samples per second. The oscilloscope was operated in 'Hi-Res' mode whereby the data are sampled at a higher frequency and then averaged on the fly into memory at the set sampling frequency.

VI.A. Smooth Insert

Figure 5 shows the surface temperature distributions with the smooth insert under quiet and noisy conditions, at freestream Reynolds numbers of 2.01 and 2.25×10^6/ft, respectively. The freestream Reynolds numbers are calculated using isentropic theory for Ludweig tubes developed by Schneider et al.[19] This theory takes into account the falling stagnation pressure and temperature inherent in a blow-down facility. The stagnation temperatures (T_0) and pressures (P_0) were T_0=418K and P_0=85 psia with the tunnel running quietly. With the noisy tunnel, T_0=424K and P_0=90 psia. The dashed red line indicates the compression corner. Figure 6a shows the streamwise temperature distribution on the centerline. The large spikes are due to the registration marks on the model surface. The compression corner is marked by the dashed black line.

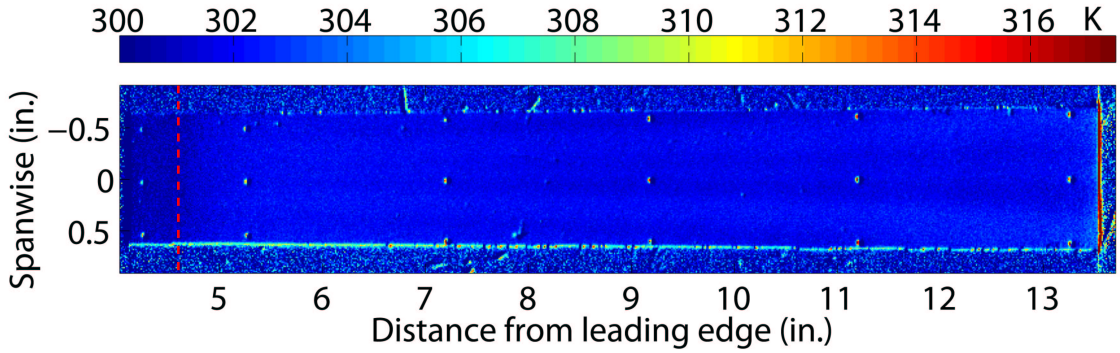

(a) Surface temperature for quiet flow, smooth insert, Re=2.01×10^6/ft

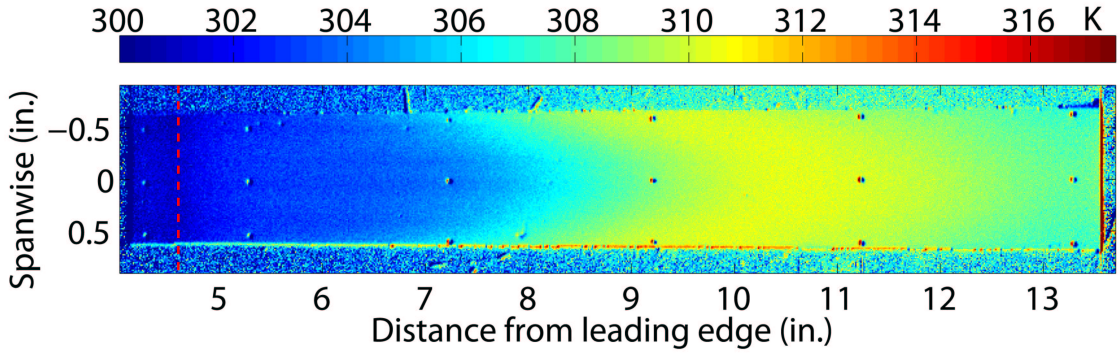

(b) Surface temperature for noisy flow, smooth insert, Re=2.25×10^6/ft

Figure 5: Surface temperature (K) under quiet and noisy conditions with smooth trip insert for Re=2.01 and 2.25×10^6/ft

Under quiet conditions, both the TSP image and the centerline temperature distribution show that the temperature increases downstream of the compression corner followed by a nearly monotonic decrease for the rest of the extent of image. This strongly suggests a laminar boundary layer over the entire length of the nylon insert. Faint streaks are also visible in the TSP image. They are most likely due to the presence of streamwise vortices near the model surface. Figure 6b shows hot-film spectra that also suggest that the boundary layer is laminar toward the aft end of the model. The low power of the low frequencies, especially when compared to the noisy tunnel data, are indicative of a laminar boundary layer. A turbulent boundary layer is expected to have much higher power, especially for low frequencies.

The results for the noisy tunnel case are very different and clearly discernible in Figures 5 and 6. After the expected rise at the corner, the temperature rises at an increased rate starting at about x=7.0 in., peaks at about x=10.6 in., and then decreases to the end of the model. This sudden rise in surface temperature is a strong indicator of transition. The high-power low-frequency signal contributions of the hot-film spectra, as well as the overall much higher magnitude power spectra when compared to the quiet case, also strongly suggest transition under noisy tunnel conditions. From Figure 6a, it is reasonable to assume that centerline transition onset takes place at around x=5.5 in. This is where the centerline surface temperature under noisy conditions significantly departs from that under quiet conditions.

It is difficult to know whether the distance from the leading edge, distance from the strip, or distance from

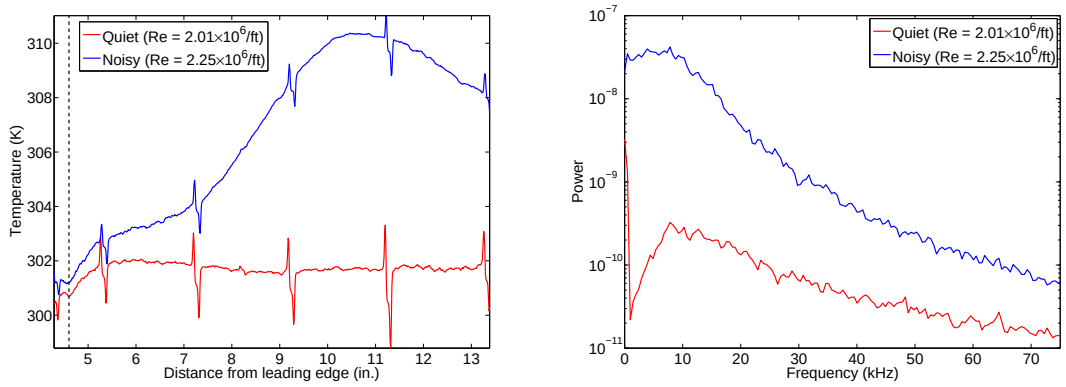

(a) Centerline temperature for quiet and noisy flow, smooth insert, Re=2.01 and 2.25×10^6/ft

(b) Hot-film spectra for smooth insert, quiet and noisy

Figure 6: Centerline temperature (K) and hot-film spectra with smooth insert under quiet and noisy conditions for Re=2.01 and 2.25×10^6/ft

the compression corner is the dominant length parameter for transition. The presence of the compression corner almost certainly has a destabilizing effect on the the boundary layer. However, it may be that the distance from the trips is the most important length factor. For the smooth-walled case, however, the distance from the nose is the most important length. Transition Reynolds numbers based on freestream conditions and all three lengths will be reported. It would be better to calculate the Reynolds number based on edge conditions, but, at present, there is no way to obtain this information.

Reducing freestream noise levels from conventional to quiet levels caused the transition Reynolds number based on distance from the nose to transition onset to increase by at least a factor of 2.2 from 1.03×10^6 to greater than 2.27×10^6. The actual value cannot be determined since the flow is laminar past the end of the model under quiet conditions at the maximum quiet Reynolds number. The transition Reynolds number based on distance from the strip increases by at least a factor of 3.2 from 0.57×10^6 to at least 1.85×10^6. Based on distance from the corner, the transition Reynolds number increases by a factor of at least 8.9 from 0.17×10^6 to 1.50×10^6.

The vortices observed under quiet flow suggest that the dominant natural, untripped transition mechanism may not be the amplification and breakdown of first or second mode waves. Spanwise spreading of the streamwise vortices indicates outward directed cross flow. Natural transition may be dominated by vorticity from the leading-edge or 3D crossflow. Transition may also be due to some complex coupling of leading edge vorticity, crossflow, and first or second mode waves with a shear layer instability above a separation bubble at the corner.[2]

VI.B. Ramp Roughness Insert

Figure 7 shows the surface temperature distribution with the ramp roughness strip under quiet and noisy conditions for Re=2.02 and 2.27×10^6/ft, respectively. For the quiet case, T_0=418K and P_0=85 psia while under noisy conditions T_0=424K and P_0=91 psia. Figure 8 shows the centerline temperatures for both cases as well as spectra computed from the surface hot film.

The significant difference between quiet and noisy flow is immediately evident from the images. For the quiet case, the temperature increases by about 6K from the compression corner to x=6 in. This is significantly higher heating than for the smooth insert case shown in Figure 6a, which increased by only about 1K downstream of the corner. This region of high heating is followed by a decrease in temperature from x=6.1 to x=8.5 in. At this point, the temperature increases sharply to a second peak at x=10.1 inches followed by a gradual decrease to the end of the model.

It seemed likely that the first temperature rise was due to the combination of compression heating as well as heating due to laminar vortices near the model surface. The decrease after the first peak was attributed to the thickening laminar boundary layer. The second temperature increase, starting at around x=8.5 in., was thought to be due to the onset of transition. Schneider[2] states that the maximum surface temperature generally corresponds to the middle of transition. Thus, at x=10.5 in., it seemed that the boundary layer

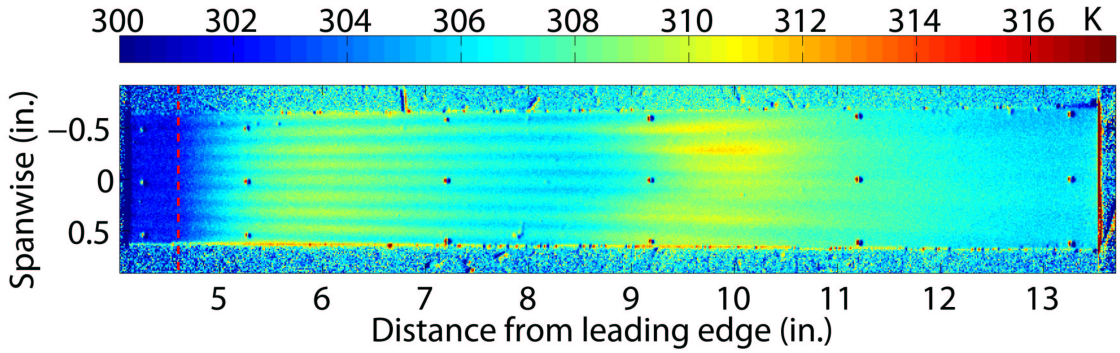

(a) Surface temperature for quiet flow, ramp trips, Re=2.02×10^6/ft

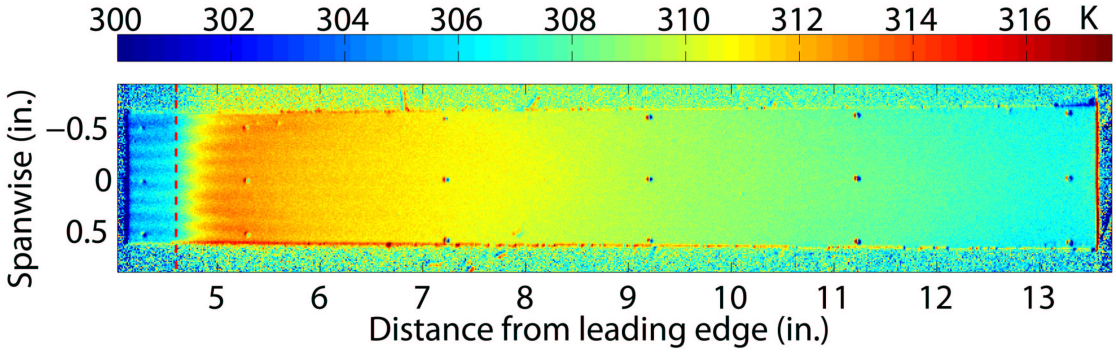

(b) Surface temperature for noisy flow, ramp trips, Re=2.27×10^6/ft

Figure 7: Surface temperature (K) distribution with ramp trips under quiet and noisy conditions for Re=2.02 and 2.27×10^6/ft

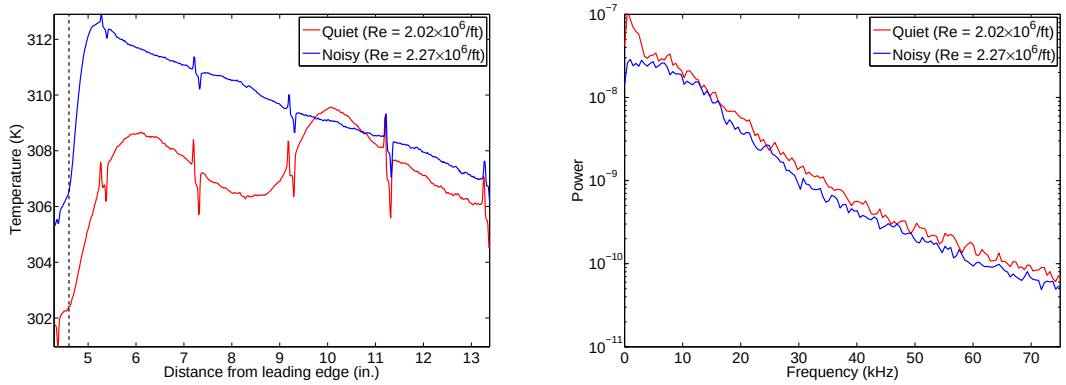

(a) Centerline temperature for quiet and noisy flow, ramp trips, Re=2.02 and 2.27×10^6/ft

(b) Hot-film spectra for quiet and noisy flow, ramp trips

Figure 8: Centerline temperature (K) and hot-film spectra with ramp trips under quiet and noisy conditions for Re=2.02 and 2.27×10^6/ft

was well on its way to being fully turbulent with the subsequent temperature decrease due to the thickening turbulent boundary layer.

Under conventional noise levels, this type of behavior is not seen. Rather, there is a sharp rise in temperature from the corner (x=4.60 in.) to x=5.5 in. This high-temperature peak is then followed by a nearly monotonic decrease to the end of the model. The sudden rise in surface temperature suggests that the boundary layer transitions just downstream of the corner. The hot-film spectra in Figure 8b supports the contention that the windward boundary layer has transitioned at the hot film (x=10.5 in.)under both quiet and noisy flow. The spectra lie almost on top of each other and show high power levels at the lower frequencies.

At present, the TSP technique is not able to provide reliable quantitative heat-transfer levels. Rather, they produce quantitative surface temperatures. In order to verify what was suspected from the TSP data, a hot wire boundary-layer probe was then used to determine the state of the windward boundary layer at different streamwise locations for the quiet runs with trip strips.

The problem with obtaining these data was that for the first hot-wire tunnel entry, the maximum quiet pressure in the BAM6QT had dropped from 95 psia to around 80 psia. This meant that hot wires could not be used at the same conditions as those in the previous measurements. It was thought that the 11% drop in initial Reynolds number would not make much difference in the results. Nevertheless, for completeness, new TSP images at the reduced quiet flow conditions were obtained for the ramp and diamond roughness inserts. Matters were further complicated when it was noted that when the tunnel was started at the somewhat reduced maximum quiet pressure, the nozzle-wall boundary layer nearly always separated for about one second some time between 1.0 and 2.5 seconds into the run. This proved to taint the TSP results for images taken during and after the separation event. Thus, images shown for the reduced quiet pressure runs were always the second image captured, generally about 0.6 seconds into the run.

Figure 9 shows the windward temperature distribution at Re=1.79×10^6/ft (T_0=427K, P_0=78 psia) for the ramp-roughness trip at the reduced maximum quiet pressure. On the TSP image, the solid yellow lines mark the streamwise locations of the hot wire measurements. Qualitatively, the temperature behaves very similarly to what was seen in Figures 7a and 8a. There is an initial temperature rise downstream of the corner followed by a decrease, a sharp rise, and then a steady decrease to the end of the model. Because of the qualitative similarities, it was decided to proceed with the hot wire measurements to determine the state of the boundary layer. The results could then be extrapolated to the TSP images at the slightly higher Reynolds numbers used earlier.

In order to accurately determine the state of the boundary layer, runs were first made with the hot wire traversing through the boundary layer in order to determine its thickness. The same hot wire was used for all three runs. Its typical square-wave frequency response was about 240 kHz. The overheat ratio based on resistances was about 1.8, making it most sensitive to mass-flux. It was a Platinum/10% Rhodium (Pt/Rh) wire with a diameter of 0.00015 in. and an L/D ratio of around 107. The hot wire was always used with the 1:1 bridge of a TSI IFA-100 constant temperature anemometer. The Textronix DPO7054 oscilloscope operating in Hi-Res mode was used to sample all hot-wire data. The sampling frequency was always 2 million samples per second.

Generally, the hot wire was placed 0.7 or 0.9 mm from the model surface. Over the course of about 6 seconds, it moved away from the model in 0.1 mm increments, stopping at each location for 200 ms. The distance from the wall at each step was then plotted against the average CTA bridge voltage. From this plot, Figure 10a, the approximate boundary layer thickness was deduced.

It should be noted that over the course of a typical run, the Reynolds number dropped by about 35%. This means that by the end of the run, when the points furthest away from the model were recorded, the boundary layer was considerably thicker than at the beginning of the run. Since the hot-wire spectra were to be computed for data at around t=0.6 sec., but the boundary layer edge was not usually crossed until about t=4.5 sec., a scaling procedure was found to approximate the boundary layer thickness at t=0.6 sec. given a measured thickness at t=4.5 sec. This scaling assumes that transition did not move over the streamwise station of interest while the probe was traversing the boundary layer. It also assumes that the thickness is proportional to the inverse square root of the Reynolds number. Thus, the approximate boundary layer thickness at t=0.6 sec. can be determined from the thickness measured at t=4.5 seconds through the following relation:

$$\frac{\delta(t=0.6)}{\delta(t=4.5)} \approx \sqrt{\frac{Re(t=4.5)}{Re(t=0.6)}} \approx \sqrt{\frac{p(t=4.5)}{p(t=0.6)}}$$

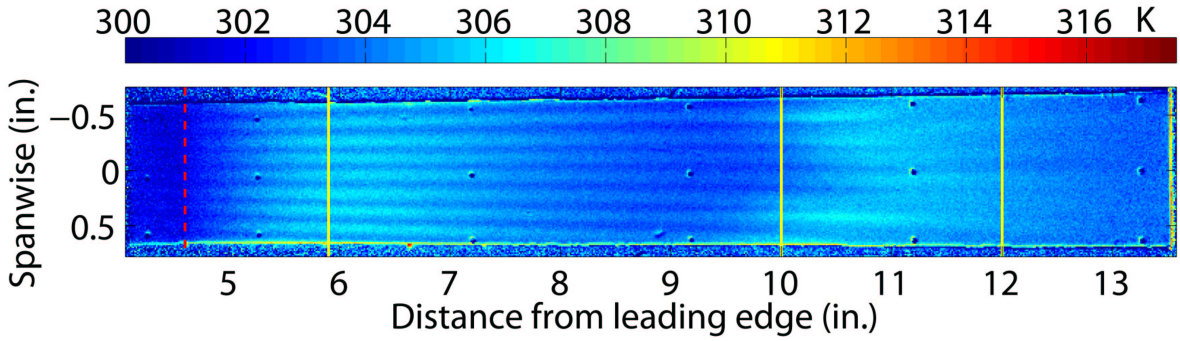

(a) Surface temperature for quiet flow, ramp trips, Re=1.79×10^6/ft

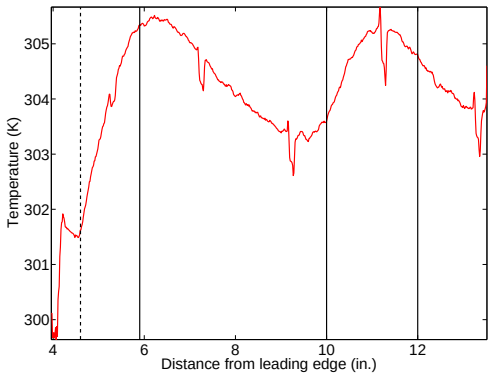

(b) Centerline temperature for quiet flow, ramp trips, Re=1.79×10^6/ft

Figure 9: Full surface and centerline temperature (K) distribution under reduced quiet flow for ramp roughnesses

where δ is the boundary layer thickness and p is the stagnation pressure. The value of this ratio is generally around 0.85. Thus, a location about 15% less than the experimentally measured edge is usually chosen as the location to place the hot wire. This ensured that the hot wire was inside the boundary layer and near the edge at the time the spectra was computed. Also, it is expected and has been experimentally shown by Rufer[20] in the BAM6QT that the amplitude of second mode instability waves is greatest near the boundary layer edge. Thus, if second mode waves were present, it was thought that they would be visible in the hot-wire spectra.

Figure 10a shows the results of the boundary-layer profile runs for streamwise locations of x=4.5, 5.9, 10.0, and 12.0 in. The large voltage spikes for locations less than 2 mm above the wall should be disregarded. These were caused by the aforementioned nozzle-wall boundary layer separation. It is not a simple matter to obtain a value for the boundary layer edge location. As can be seen, the voltage gradually approaches a peak value and then generally decreases again. An approximate value for the edge location is all that could be readily obtained. Finding a more accurate value for the boundary layer edge at a specific time was beyond the scope of the current investigation.

Figure 10b shows the power spectra at Re≈1.8×10^6/ft for streamwise hot wire locations of x=5.9, 10.0, and 12.0 in. as well as spectra computed for the x=10.0 in. pre-run signal. The corresponding distances above the model surface were 2.7, 3.0, and 3.0 mm, respectively. The spectra were computed over a 200 msec interval. As much as was possible, they were computed over a portion of the signal that did not have any turbulent bursts in it. Each spectra was the average of 100 FFTs, with each FFT computed from 4000 data points. Welch's averaged, modified periodogram method with a Hamming window was used.

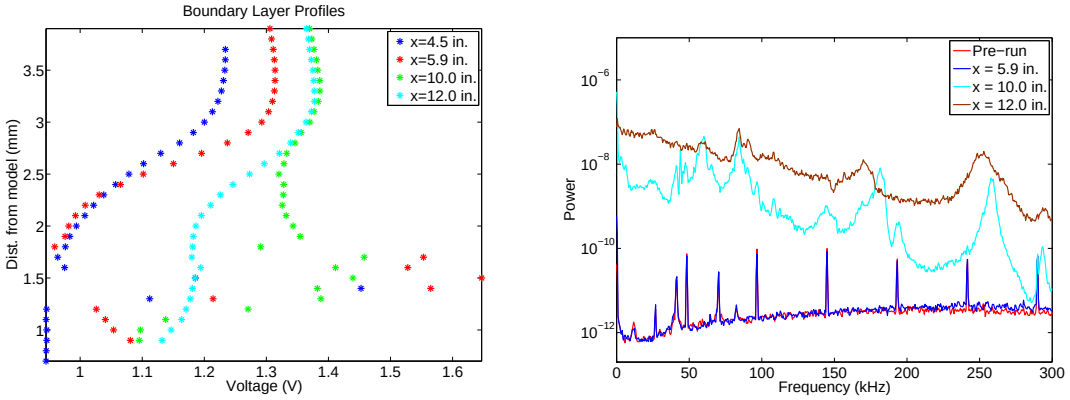

(a) Boundary layer profiles at reduced maximum quiet pressure

(b) Hot wire spectra for ramp roughness, Re≈1.8×10^6/ft

Figure 10: Boundary layer profiles and hot-wire spectra for ramp roughness

As can be seen in Figure 10b, the spectrum when the hot wire was located at x=5.9 in. (very near the local peak in the centerline temperature) falls nearly on top of the pre-run spectrum. This indicates that there are very few disturbances in the boundary layer at that location and that it is laminar, as was previously suspected from the paints data. The spectrum for x=10.0 in. is very different from that at x=5.9 in. The location x=10.0 in. is just downstream of where the centerline temperature began to increase for the second time. It was suspected that this location was near to the midpoint of transition. The spectrum supports this notion. The power levels, especially for the lower frequencies, are orders of magnitude higher than the pre-run and x=5.9 in. spectra. It appears that the boundary layer at x=10.0 in. may not be completely turbulent, but there are significant disturbances present at that location. The spectrum at x=12.0 in., where it was suspected that the boundary layer had become fully turbulent, shows power levels generally at least a factor of two greater than for the x=10.0 in. case. These high levels of broadband noise are due to a turbulent boundary layer at x=12.0 in.

Because the hot wire and TSP data agree about the state of the boundary layer at the reduced quiet pressure, conclusions can be drawn from the TSP images at higher pressure even though there are no supporting hot-wire measurements. Transition is taken to be at about x=8.25 in. under quiet conditions at P_0=85 psia (Figure 8a). It happens immediately downstream of the compression corner under noisy conditions. Reducing freestream noise levels from conventional to quiet levels caused the transition Reynolds number based on distance from the nose to increase by a factor of 1.6 from 0.87×10^6 to 1.39×10^6. The

transition Reynolds number based on distance from the strip increases by a factor of 2.4 from 0.40×10^6 to 0.97×10^6. Based on distance from the corner, the transition Reynolds number increases from 0 to 0.68×10^6. Under the reduced quiet pressure conditions, transition was taken to be at x=9.5 in. For the three different length parameters, this gave transition Reynolds numbers 1.42, 1.05, and 0.79×10^6, respectively.

This large effect of freestream noise levels on transition is not altogether surprising. The wake behind large roughness elements is often unstable. When freestream noise levels are elevated, increased disturbance levels can be introduced into the unstable wake via a receptivity process. The growth of wake instabilities thus starts at a higher level which can then lead to earlier breakdown and transition of the boundary layer.[21]

VI.C. Diamond Roughness Insert

A similar set of experiments was carried out with the diamond trips in the model. Figure 11 shows the surface temperature distribution with the diamond roughness strip under quiet and noisy conditions for Re=2.05 (T_0=422K, P_0=88 psia) and 2.24×10^6/ft (T_0=424K, P_0=89 psia), respectively. Figure 12 shows the centerline temperature for both cases as well as spectra computed from the surface hot film.

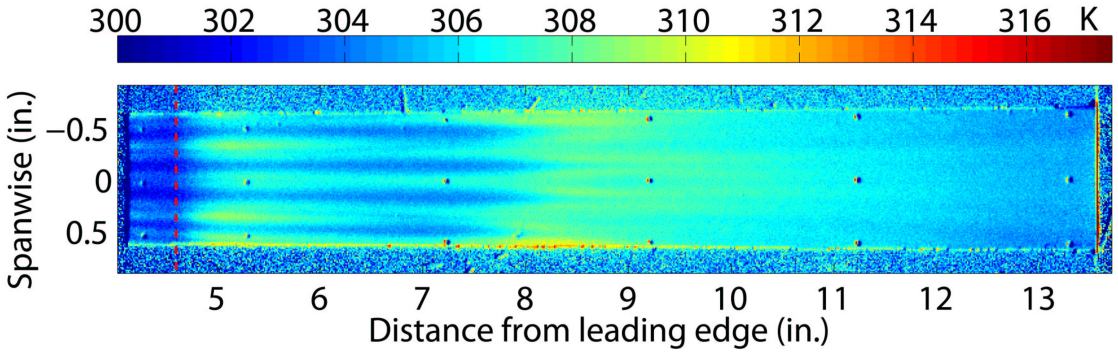

(a) Surface temperature for quiet flow, diamond trips, Re=2.05×10^6/ft

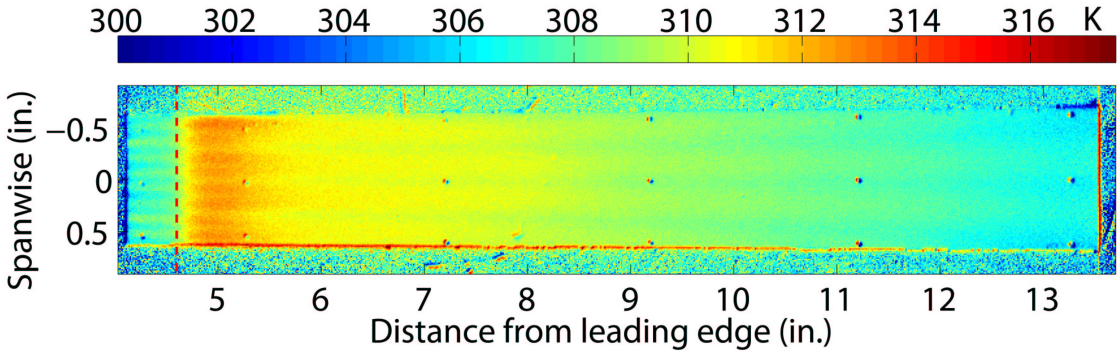

(b) Surface temperature for noisy flow, diamond trips, Re=2.24×10^6/ft

Figure 11: Surface temperature (K) with diamond trips under quiet and noisy conditions for Re=2.05 and 2.24×10^6/ft

As the figures show, qualitatively, the surface temperature behaves very similarly to the ramp roughness case. Under quiet conditions, just downstream of the compression corner, there is an initial temperature rise. This is followed by a decrease, another sharp rise, and then a gradual reduction of the surface temperature. Additionally, high-temperature streaks are visible from upstream of the corner to the second temperature rise. The locations of the temperature peaks are upstream of the ramp roughness case, however, occurring at x=5.4 and 8.4 inches instead of x=6.1 and 10.1 inches, respectively.

Due to the qualitative similarities to the ramp roughness case, it was thought that the first temperature rise was again due to compression heating at the corner and the presence of laminar vortices near the model surface. The second peak was again believed to be due to transition. The hot-film spectra support this theory for the runs at 95 psia initial stagnation pressure, showing high power levels in the low frequency band.

Again, due to the reduced maximum quiet pressure for the later hot-wire experiments in the BAM6QT,

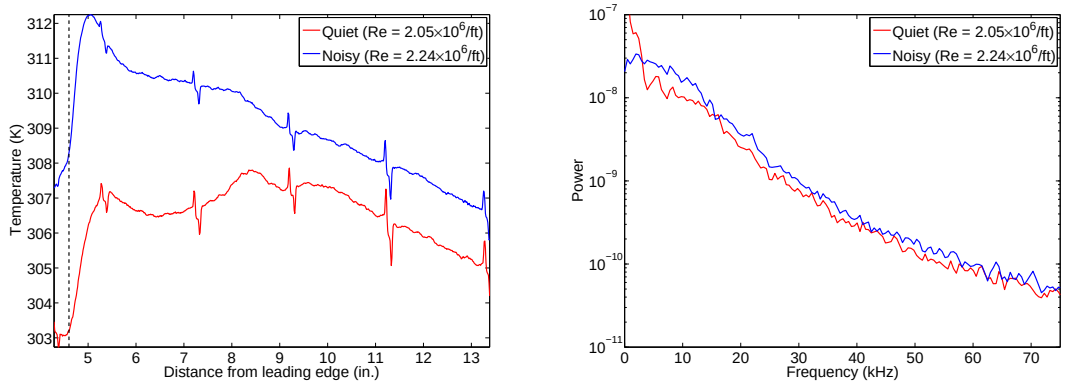

(a) Centerline temperature for quiet and noisy flow, diamond trips, Re=2.05 and 2.24×10^6/ft

(b) Spectra for noisy and quiet flow with diamond roughness

Figure 12: Centerline temperature (K) distribution and hot-film spectra with diamond trips under quiet and noisy conditions for Re=2.05 and 2.24×10^6/ft

a TSP image was again taken under reduced pressure conditions before checking the boundary layer state with a hot wire. Here, Re=1.78×10^6/ft, T_0=427K, and P_0=78 psia. The surface temperature distribution can be seen in Figure 13a. The dashed red line is the compression corner and the solid yellow lines are the locations for which spectra were computed. A brief comparison shows very similar behavior to that of Figure 11a, the TSP image for quiet flow at 95 psia. The locations of the temperature peaks are moved somewhat downstream from the similar peaks observed at Re=2.05×10^6/ft, but the qualitative similarities are sufficient reason to believe that the boundary layer behaves in the same way as for the higher Reynolds number case.

Figure 14 shows hot wire spectra at x=4.2, 5.5, 8.0, and 12.0 in. for distances from the model of 3.0, 2.7, 2.8, and 3.0 mm, respectively. It should be noted that x=4.2 in. is 0.4 in. upstream of the compression corner. A power spectrum was also computed for 200 ms of pre-run data for comparison.

It was at first surprising to find that the boundary layer was thicker at x=4.2 in. than for locations further downstream. Given the unique nature of the flow, however, this is not too difficult to explain. The flow at these locations is downstream of large roughness elements. In addition, it seems likely that there is a separation bubble at the compression corner. The effects and extent of such a separation, upstream and downstream, are not fully understood. Boundary layer separations in hypersonic flow have been shown to extend up to 100 boundary layer thicknesses upstream of the initial cause of the separation.[22] It may also be that downstream of the reattachment point it takes a considerable distance for the boundary layer to fully process the effects of the separation. Also, it is clear from the vortices in the TSP images that there is some outward-directed crossflow. This certainly affects the boundary layer thickness.

The power of the lower-frequency disturbances in the boundary layer at x=4.2 in. are not quite as low in magnitude as the pre-run spectra. For higher frequencies, they are of the same order. At x=5.2 in., about 0.6 in. downstream of the compression corner, for frequencies from 20-75kHz and 200-300kHz, the power levels are very similar to those at x=4.2 in. From 75-200kHz, the power levels were generally around an order of magnitude higher at x=5.2 in. than at x=4.6 in. The spectra at x=8.0 and 12.0 in. show still higher power levels that are very similar in magnitude to each other, with the x=8.0 in. case exhibiting the slightly lower power levels of the two.

These data again support what the TSP images suggest. Due to lower power levels at x=4.2 and 5.5 in. compared to locations further downstream, it is concluded that the boundary layer is laminar at those locations. However, the power levels are higher and much more uneven than for the ramp roughness insert. This is not surprising though. The diamond roughnesses are 0.060 in. high, while the ramps have a maximum height of 0.030 in. The larger roughness gives rise to greater disturbances in the boundary layer, evidenced by higher and more uneven power levels in the power spectra. The trends in the spectra at x=8.0 and 12.0 in. suggest a turbulent boundary layer. This is somewhat surprising for the x=8.0 in. location. From Figure 13b, this location is just downstream of onset of the second temperature rise. It was thought that this second rise marked the onset of transition. As such, generally higher power levels were expected, but not to

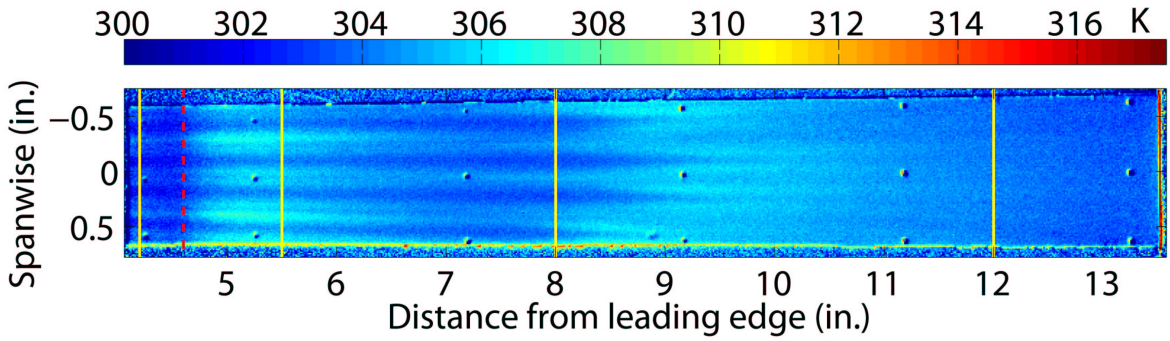

(a) Surface temperature for quiet flow, diamond trips, Re=1.78×10^6/ft

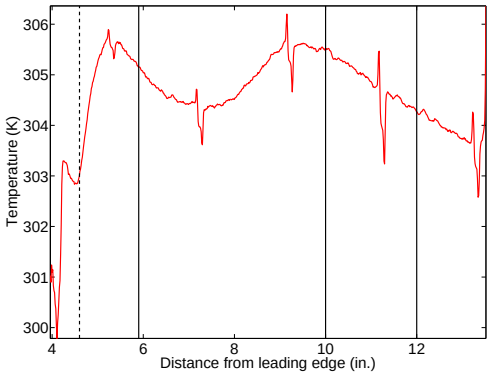

(b) Centerline temperature for quiet flow, diamond trips, Re=1.78×10^6/ft

Figure 13: Full surface and centerline temperature (K) distribution under reduced quiet flow for diamond roughnesses

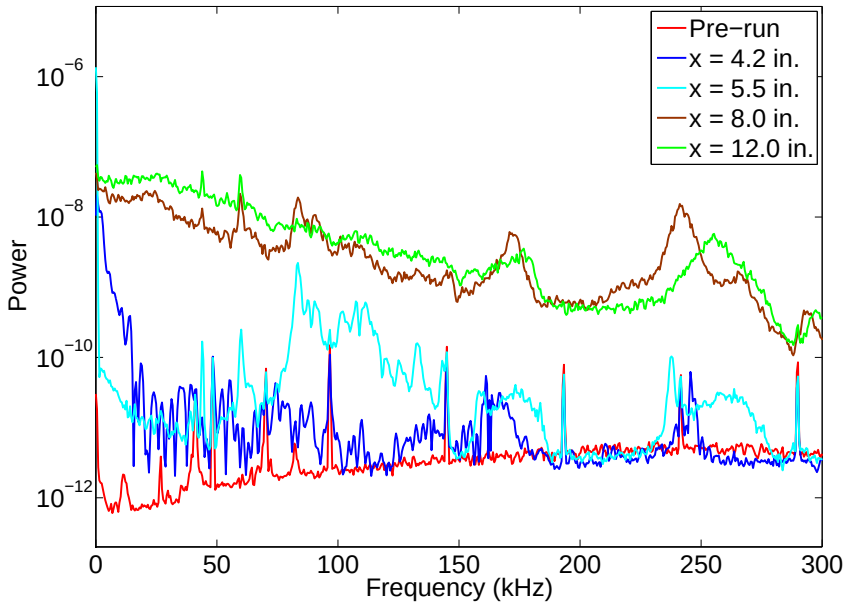

Figure 14: Hot wire spectra for diamond roughness

the degree as those that were observed. It is possible that either the larger roughnesses and the resultant large disturbances cause the boundary layer to complete transition over a very short streamwise distance or that the boundary layer has not completely transitioned at x=8.0 in. At x=8.0 in., the power levels are lower than those at x=12.0 in. for all frequencies, signifying that it may not yet be entirely turbulent.

Transition onset is observed to occur at x=6.5 in. under quiet conditions. Under noisy conditions, a fully turbulent boundary layer is seen just downstream of the corner. Reducing freestream noise levels from conventional to quiet levels caused the transition Reynolds number based on distance from the nose to increase by a factor of 1.3 from 0.86 million to 1.11 million. The transition Reynolds number based on distance from the strip increases by a factor of 1.7 from 0.40 million to 0.69 million. Based on distance from the corner, the transition Reynolds number increases from 0 to 0.39 million. Under the reduced quiet pressure conditions, transition was taken to be at x=7.2 in. For the three different length parameters, this gave transition Reynolds numbers of 1.07, 0.70, and 0.45×10^6, respectively.

This increase is not as substantial as observed with the ramp trips. This result is not surprising, however, given the larger height of the diamond trips and the fact that both the ramp and diamond trips induced transition at the corner and, apparently, not upstream of it under noisy conditions. Thus the diamond roughness should serve to introduce much larger disturbances into the boundary layer and cause earlier transition under quiet conditions.

VII. Conclusions

The effect of tunnel noise on natural and roughness-dominated transition was clearly seen on the 20%-scale X-51A forebody model in the BAM6QT. On the smooth model, no transition was observed in the TSP under quiet flow at Re=2.01×10^6/ft. When the tunnel was noisy, however, a clear transition front was seen by about x=7 in. Although no hot-wire measurements were made to confirm these conclusions, hot-wire measurements with transition induced by roughness strips support these conclusions. Reducing freestream noise from conventional to quiet levels increased the transition Reynolds number by a factor of at least 2.2, 3.2, and 8.9, where the length parameters were the distance from the nose, distance from the strip, and distance from the corner, respectively.

With the ramp roughness strip in the model under quiet conditions at Re=1.79×10^6/ft, an initial temperature rise downstream of the compression corner was observed and attributed to laminar vortex heating. Further downstream, at about x=8.25 in., the onset of transition was observed with TSP and confirmed by hot-wire spectra. Under noisy conditions at Re=2.27×10^6/ft, the ramp roughnesses caused transition almost immediately downstream of the corner. Reducing freestream noise from conventional to quiet levels increased the transition Reynolds number by a factor of 1.6 and 2.4 where the length parameters were the distance from the nose and distance from the strip, respectively. When based on the length from the corner, the transition Reynolds number increased from 0.0 to 0.68 $\times10^6$.

The diamond roughness insert provided results qualitatively similar to those of the ramp roughness. Under quiet conditions at Re=1.78×10^6/ft, the location of peak laminar vortex heating as well as peak transitional heating was found to move upstream by around 2 in. when compared to the ramp roughness results. Under noisy conditions at Re=2.24×10^6/ft, the boundary layer transitioned immediately downstream of the compression corner. Reducing freestream noise from conventional to quiet levels increased the transition Reynolds number by a factor of 1.3 and 1.7 where the length parameters were the distance from the nose and distance from the strip, respectively. When based on the length from the corner, the transition Reynolds number increased from 0.0 to 0.39 $\times10^6$.

It is well known that tunnel noise can have a profound effect on transition. In addition, a few previous experiments have shown an effect of tunnel noise on roughness-induced transition. However, to the author's knowledge, the present paper reports the first hypersonic measurements of roughness-induced transition under low noise levels that are comparable to flight.

If the trip size for the X-51A flight vehicle were based on results from wind tunnels with conventional noise levels, it is possible that the trips would be undersized. Thus, transition on the vehicle would be delayed too far under the quiet conditions of the atmosphere. Clearly, quiet tunnel results should be used to help determine the heights of such trips. However, it is not clear how to account for facility noise nor how to scale the trip sizes from facility to facility to flight. Further research is needed to develop methods of predicting the effect of roughness elements. The effect of tunnel noise should be one part of these improved prediction methods.

Acknowledgments

This research is funded by AFOSR under grant FA9550-06-1-0182. Fabrication of the model was supported in part by the Boeing Company.

References

[1]Schneider, S. P., "Laminar-turbulent transition on reentry capsules and planetary probes," *Journal of Spacecraft and Rockets*, Vol. 43, No. 6, 2006, pp. 1153–1173.

[2]Schneider, S. P., "Hypersonic laminar-turbulent transition on circular cones and scramjet forebodies," *Progress in Aerospace Sciences*, Vol. 40, 2004, pp. 1–50.

[3]Beckwith, I. E. and Miller III, C., "Aerothermodynamics and transition in high-speed wind tunnels at NASA Langley," *Annual Review of Fluid Mechanics*, Vol. 22, 1990, pp. 419–439.

[4]Schneider, S. P., "Effects of high-speed tunnel noise on laminar-turbulent transition," *Journal of Spacecraft and Rockets*, Vol. 38, No. 3, 2001, pp. 323–333.

[5]Schneider, S. P., "Flight data for boundary-layer transition at hypersonic and supersonic speeds," *Journal of Spacecraft and Rockets*, Vol. 36, No. 1, 1999, pp. 8–20.

[6]Wilkinson, S. P., Anders, S. G., and Chen, F.-J., "Status of Langley quiet flow facility developments," AIAA Paper 94-2498, June 1994.

[7]Beckwith, I., Creel, T., Chen, F., and Kendall, J., "Freestream noise and transition measurements on a cone in a Mach-3.5 Pilot Low-Disturbance Tunnel," Technical Paper 2180, NASA, September 1983.

[8]Blanchard, A. E., Lachowicz, J. T., and Wilkinson, S. P., "NASA Langley Mach 6 quiet wind-tunnel performance," *AIAA Journal*, Vol. 35, No. 1, January 1997, pp. 23–28.

[9]Schneider, S. P., "The development of hypersonic quiet tunnels," AIAA Paper 2007–4486, June 2007.

[10]Schneider, S. P. and Haven, C. E., "Quiet-flow Ludwieg tube for high-speed transition research," *AIAA Journal*, Vol. 33, No. 4, April 1995, pp. 688–693.

[11]Juliano, T. J., Swanson, E. O., and Schneider, S. P., "Transition research and improved performance in the Boeing/AFOSR Mach-6 Quiet Tunnel," AIAA Paper 2007-0535, January 2007.

[12]Schneider, S. P. and Juliano, T. J., "Laminar-turbulent transition measurements in the Boeing/AFOSR Mach-6 Quiet Tunnel," AIAA Paper 2007-4489, June 2007.

[13]Creel, T., Beckwith, I., and Chen, F., "Transition on Swept Leading Edges at Mach 3.5," *Journal of Aircraft*, Vol. 24, No. 10, October 1987, pp. 710–717.

[14]Ito, T., Randall, L. A., and Schneider, S. P., "Effect of noise on roughness-induced boundary-layer transition for scramjet inlet," *Journal of Spacecraft and Rockets*, Vol. 38, No. 5, September 2001, pp. 692–698.

[15]Liu, T. and Sullivan, J., *Pressure and Temperature Sensitive Paints*, Springer, New York, 2005.

[16]Matsumura, S., Schneider, S. P., and Berry, S. A., "Streamwise vortex instability and transition on the Hyper-2000 scramjet forebody," *Journal of Spacecraft and Rockets*, Vol. 42, No. 1, 2001, pp. 78–89.

[17]Berry, S. A., Auslender, A. H., Dilley, A. D., and Calleja, J. F., "Hypersonic boundary-layer trip development for Hyper-X," *Journal of Spacecraft and Rockets*, Vol. 38, No. 6, 2001, pp. 853–864.

[18]Schmisseur, J., Young, J., and Schneider, S. P., "Measurements of boundary-layer transition on the flat sidewall of a rectangular Mach 4 quiet-flow nozzle," AIAA Paper 96–0852, Jan. 1996.

[19]Schneider, S. P., Collicott, S. H., Schmisseur, J., Ladoon, D., Randall, L. A., Munro, S. E., and Salyer, T. R., "Laminar-turbulent transition research in the Purdue Mach-4 Quiet-Flow Ludwieg tube," AIAA Paper 96–2191, June 1996.

[20]Rufer, S. and Schneider, S. P., "Hot-wire measurements of instability waves at Mach 6," AIAA Paper 2006–3054, June 2006.

[21]Schneider, S. P., "Effects of roughness on hypersonic boundary-layer transition," AIAA Paper 2007–0305, Jan. 2007.

[22]Skoch, C., Schneider, S. P., and Borg, M. P., "Disturbances from shock/boundary layer interactions affecting upstream hypersonic flow," AIAA Paper 2005–4897, June 2005.